Antiproliferative activity of di-2-pyridylhydrazone dithiocarbamate acetate partly involved in p53 mediated apoptosis and autophagy

TINGTING WANG[1,2*], YOUXUN LIU[1*], YUN FU[1], TENGFEI HUANG[1], YUN YANG[1], SHAOSHAN LI[3] and CHANGZHENG LI[1,2]

[1]Department of Molecular Biology and Biochemistry, [2]Henan Collaborative Innovation Center of Molecular Diagnostics and Laboratory Medicine, Xinxiang Medical University; [3]Department of Surgery, The Third Affiliated Hospital of Xinxiang Medical University, Xinxiang, Henan 453003, P.R. China

Received July 11, 2017; Accepted October 4, 2017

DOI: 10.3892/ijo.2017.4149

Abstract. Cancer cells have higher demand of iron and copper ions for growth, disturbing the metal's homeostasis can inhibit proliferation of cancer cell. Dithiocarbamates possessing excellent metal chelating ability and antitumor activity are considered as candidates in chelation therapy, however, their antitumor molecular mechanisms remain to be elucidated. In the present study, a dithiocarbamate derivative, di-2-pyridylhydrazone dithiocarbamate s-acetic acid (DpdtaA) was prepared to address the issue whether the molecular mechanism behind biological behavior showed by dithiocarbamate was p53 mediated. The proliferation inhibition assay showed that DpdtaA exhibited excellent antiproliferative effect for hepatocellular carcinoma (IC_{50}= 3.0±0.4 μM for HepG2, 6.1±0.6 μM for Bel-7402 cell). However, in the presence of copper ion, the antiproliferative activity of DpdtaA significantly attenuated (~3-fold for HepG2) due to formation of copper chelate. The ROS assay revealed that the antiproliferative activity of DpdtaA correlated with ROS generation. Western blotting demonstrated that DpdtaA could upregulate p53 via downregulating the Mdm2, accordingly leading to changes of bcl family proteins, indicating that a p53-dependent intrinsic apoptosis was partly involved. Simulation from molecular docking hinted that DpdtaA could disrupt interaction between p53 and Mdm2, indicating the disruption might also contribute to the upregulation of p53. The alternations in lysosome membrane permeability and acidic vacuoles as well as LC3-II upregulation indicated that autophagy was involved. The copper addition led to significantly attenuate biological activity of DpdtaA, with few dithiocarbamates, but the mechanism in apoptosis induction was not altered except for weaker ability.

Correspondence to: Professor Changzheng Li, Department of Molecular Biology and Biochemistry, Xinxiang Medical University, Xinxiang, Henan 453003, P.R. China
E-mail: changzhenl@yahoo.com

Professor Shaoshan Li, Department of Surgery, The Third Affiliated Hospital of Xinxiang Medical University, Xinxiang, Henan 453003, P.R. China
E-mail: shaoshanlioo1@sina.com

*Contributed equally

Key words: di-2-pyridylhydrazone dithiocarbamate s-acetic acid, antiproliferative activity, apoptosis, p53, autophagy, antagonistic effect, copper complex, ROS, mechanism

Introduction

Cancer is one of most deadly diseases, while hepatocellular carcinoma (HCC) lies in the third position in cancer caused deaths. Resection is often used for certain patients, but mostly transiently, the reason is lack of clinical marker for surgeon due to tumor metastasis (1). Therefore, the chemotherapy is still important procedure in clinical practice, but the side-effect and drug-resistance limit it widely use. Looking for novel drug with highly selectivity and efficiency is an urgent task for medical research. It has been recognized that tumor microenvironment plays an important role in the metastasis process (1,2), the metalloenzymes, such as MMPs in tumor environment are required to degrade extracellular matrix, thus, the metalloproteases are also considered as targets in metastasis inhibition (3). Copper, iron and zinc are essential trace metal elements for most organisms, those metal ions present in either in metalloenzymes or metal labile pools. Generally, cancer cell has higher demand for iron compared to normal cell, meanwhile to acquire metastatic phenotype the vascularization is also required for tumor cell escaping from local site, the copper ion has critical role during the vascularization, copper-lowering directly results in inhibition of angiogenesis and cancer cell growth (4,5), therefore, use of chelators for cancer treatment is prospective strategy.

Dithiocarbamates are an important class of sulfur-containing compounds with various applications in medicine, such as diethyldithiocarbamate and brassinin. They have been used for the treatment of bacterial, fungal infections, AIDS

and cancer (6). To achieve better biological activity, many studies of structural modification on compounds have been conducted (7-11), some of which were found to have excellent antitumor activity *in vitro* and *in vivo*. Due to many metal complexes exhibiting significant antiproliferative activity in clinic, many metal complexes of dithiocarbamates have been prepared and investigated in antitumor activity. Some of them, as such gold, platinum and palladium complexes showed prospective use in cancer therapy and entered preclinical observation (12,13). Preliminary mechanistic studies revealed that dithiocarbamate derivatives can be inhibitors of nuclear factor kappa B (14), proteasome inhibitor (11), DNA intercalator, and inactivator of numerous metal-containing enzymes (15). However, whether the antiproliferative activity of dithiocarbamate correlates with p53 activation remains to be elucidated (16-18). To gain more details of dithiocarbamate against tumor cells, in the present study we made a novel dithiocarbamate derivative (dipyridylhydraone dithiocarbamate s-acetic acid, DpdtaA), which contain both a heterozygous coordination unit and S-alkylated group. The new derivative may achieve higher stability and less undesirable consequences due to not directly inactivating enzymes that cell growth required. To address the role of p53 in antiproliferative activity of the dithiocarbamate, p53 expression at different conditions was assessed. The preliminary mechanistic study revealed that the antiproliferative effect of the new dithiocarbamate derivative was partly involved in ROS production, p53 mediated apoptosis and autophagy. The p53 upregulation was attributed to downregulation of Mdm2 (mouse double minute 2 homolog), and potent disruption of the interaction between p53 and Mdm2 based on molecular docking. Furthermore, p53 activation led to alteration in apoptosis-related proteins and autophagy after exposure of the agent to the cell lines. Besides, copper ion could attenuate cytotoxicity of DpdtaA, which was similar to previously observations.

Materials and methods

General information. MTT, di-2-pyridylketone, 3-methyladenin (3-MA), Pifithrin-α, RPMI-1640 and other chemicals were purchased from Sigma-Aldrich. LC3 antibody was obtained from Proteintech Group (Wuhan, China); antibodies p53, caspase-8, β-actin, cytochrome *c*, Bax, Mdm2 and Bcl-2 were purchased from Wuhan Boster Biological Technology, Ltd. (Wuhan, China).

Preparation of di-2-pyridylhydrazone dithiocarbamate s-acetic acid (DpdtaA). DpdtaA (generated by ACDLabs: 3-[({2-[di(pyridin-2-yl)methylidene] hydrazinyl} carbonothioyl) sulfanyl] acetic acid) was made by three-step reactions as indicated in Fig. 1: the first two steps were as previously described (19). In addition, the final product (DpdtaA) was prepared by reaction of di-2-pyridylhydrazone dithiocarbamate (1 mmol) with 2-bromo acetic acid in absolute ethanol (5 ml), the yellow solid was filtered and washed with ethanol. TLC tracing (ethyl acetate/petroleum ether = 3:1) showed the reaction completed. Following a flash chromatography the purity of the compound was achieved to 98%. Yield: 80%; mp: 148.6˚C; composition: $C_{14}H_{12}N_4O_2S_2$; ^{1}HNMR (Bruker, D_6-DMSO): 8.86 (d, H, J = 4 Hz), 8.64 (d, H, J = 4 Hz), 8.02 (m, 3H, J = 4, 8 Hz), 7.63 (m, 2H, J = 8 Hz), 7.55 (ddd, H, J = 4, 8 Hz), 4.12 (s, 2H). ^{13}CNMR: 199.25, 169.87, 155.09, 151.14, 149.20, 148.94, 145.43, 138.24, 137.92, 128.04, 125.72, 124.93, 123.96, 36.80. IR (cm^{-1}): IR (KBr, cm^{-1}): 3088, 1709, 1584, 1458, 1435, 1417, 1393, 1326, 1292, 1234, 1202, 1188, 1127, 1058, 1018, 959, 905, 802, 791, 750, 695, 654, 640, 596, 472. ESI-MS (microTOF-Q III, Bruker): m/z: 371.0043 (M+K, calcd: 371.00389).

Cytotoxicity (MTT) assay. A 10 mM DpdtaA in 70% dimethyl sulfoxide (DMSO) was diluted to the required concentration with culture. The copper complex was prepared by mixing DpdtaA with $CuCl_2$ (at high concentration) based on 1:1 molar ratio and diluted to required concentration with DMSO. The MTT assay was conducted as previously described (20). Briefly, the HepG2 ($5x10^3$/ml) cells were seeded equivalently into 96-well plate and the various amount of DpdtaA (or its copper complex) was added after the cells adhered. Following 48-h incubation at 37˚C in a humidified atmosphere of 5% CO_2, 10 μl MTT solution (5 mg/ml) was added to each well, and incubated further for 4 h. After removing the cell culture, 100 μl DMSO was added in each well to dissolve the formed formazan. The absorption of the solution that was related to the number of live cells was performed on a microplate reader (MK3; Thermo Fisher Scientific, Waltham, MA, USA) at 490 nm. Percent growth inhibition was defined as percent absorbance inhibition within appropriate absorbance in each cell line. The same assay was performed in triplicate. Morphologic study was conducted under inverted microscope (Shanghai Batuo Instrument Co., Ltd., Shanghai, China), the photographs of HepG2 cells exposed to DpdtaA (1.56 or 3.12 μM DpdtaA or DpdtaA-Cu for 24 or 48 h were recorded (objective size: 10x20).

ROS detection in vitro and in vivo. ROS production assessment was conducted as previously reported (21). Briefly, H_2DCF-DA was first converted to dichlorofluorescin (DCF) by NaOH, following neutralization, the hydrolysate was used for the assay. Reaction system contained either single reagent or multicomponent in 50 mM sodium phosphate buffer (pH 7.4) with total 4 ml volume, i.e., 0.4 μM DCF, or with 6.25 μM $(NH_4)_2Fe(SO_4)_2$ (or $CuCl_2$ or DpdtaA) and 200 μM H_2O_2 (1 mM) for the Fenton reactions. The fluorescence was detected by a FC-960 spectrofluorimeter (excitation at 488 and emission at 525 nm; Shanghai Lengguang Technology Co., Ltd., Shanghai, China) in a 10-min time course at room temperature.

The intracellular ROS assay was measured as company recommended (Beyotime Institute of Biotechnology, Beijing, China). Briefly, ~10^6 HepG2 cells were collected and washed by phosphate-buffered saline (PBS), then the cells were stained by H_2DCF-DA in serum-free culture medium for 30 min, followed by washing of serum-free culture to remove excess H_2DCF-DA. Then, 100 μl the cell suspension was transferred to individual PCR tube and the test compound (or positive control) was added, following 1-h incubation, the cell suspension was used directly for ROS detection on a FC-960 spectrofluorimeter (excitation at 488 nm and emission at 525 nm; Shanghai Lengguang Technology).

Western blot analysis. Briefly, 1x10^7 HepG2 cells treated with or without the DpdtaA or DpdtaA-Cu were scraped off in lysis buffer (50 mM Tris-HCl, pH 8.0, 150 mM NaCl, 1.0% NP-40, 10% glycerol and protease inhibitors) and subjected to sonication, following spin down by centrifugation at 14,000 x g. The clear supernatant was stored at -80˚C. The protein concentration was determined using a colorimetric Bio-Rad DC protein assay on a microplate reader MK3 at 570 nm. Proteins (50 μg) were separated on a 13% sodium dodecyl sulfate-polyacrylamide gel at 200 V for 1 h. The separated proteins were subsequently transferred onto a PVDF membrane at 60 V for 1 h. The membrane was washed three times with Tris-buffered saline (TBS) and was then blocked for 2 h in TBS containing 0.1% Tween-20 and 5% non-fat skimmed milk. The membrane was incubated at 4˚C overnight with the primary monoantibody used at a dilution of 1:300 in TBS plus 0.1% Tween-20 (TBST). The membrane was washed several times with TBST and was subsequently incubated with HRP-conjugated secondary antibody (1:2,000 in TBST) for 1 h at room temperature. After another wash of the membrane with TBST, the protein bands were detected using a super sensitive ECL solution (Wuhan Boster Biological Technology), and visualized on an Amersham Imager 600 (GE Healthcare Life Sciences, Fairfield, CT, USA).

Cytoflow analysis of apoptosis. Cells were seeded into a 6-well flask and treated as described above for the cell viability assay. The cells were treated with different concentrations of the agents (0.78 and 1.56 μM DpdtaA or 3.12 and 6.25 μM DpdtaA-Cu) for 24 h. Then the cell culture was removed, following PBS washing, trypsin digestion, finally the Annexin V and propidium iodide (a kit from Dojindo Laboratories, Kumamoto, Japan) were added as recommended by the company. The stained cells were subjected to cytoflow analysis.

Molecular docking studies. The structure of human type MDM2 (3jzk) was obtained from the RCSB Protein Data Bank. The structure of DpdtaA was generated by Chemdraw (Chemdraw Ultra 8.0; CambridgeSoft, Cambridge, MA, USA). The energy minimization was conducted by Chem3D (Ultra 8.0; CambridgeSoft). PyMol and LigPlot displayed the conformation, interaction between bound ligands and residue around the binding cavity (22,23).

Molecular docking studies were performed by AutoDock Vina and AutoDock Tools based on the recommended procedure (24). Grid box was set to the center of Yin model, and the grid box size for DpdtaA was set to 22, 24 and 28 for x-, y- and z-axes, respectively. The DpdtaA was set as a flexible ligand by using the default parameters of the AutoDock Tools. The optimal conformation of the ligand was generated by AutoDock Vina.

DpdtaA and its copper complex induced autophagy and LMP. Cells were seeded into a 24-well flask and treated as described above in the cell viability assay. The cells were treated with different concentrations of the agents (0.78 and 1.56 μM DpdtaA or 3.12 and 6.25 μM DpdtaA-Cu) for 24 h. For detection of the acidic cellular compartment, acridine orange (or LysoTracker Red; Invitrogen) was used, which emits bright red fluorescence in acidic vesicles but green fluorescence in the cytoplasm and the nucleus. After treatment of the cells with the agent, acridine orange was added at a final concentration of 1 μg/ml (the concentration of LysoTracker Red, as recommended) for a period of 15 min. Following PBS washing, the fluorescent micrographs were captured using an inverted fluorescence microscope.

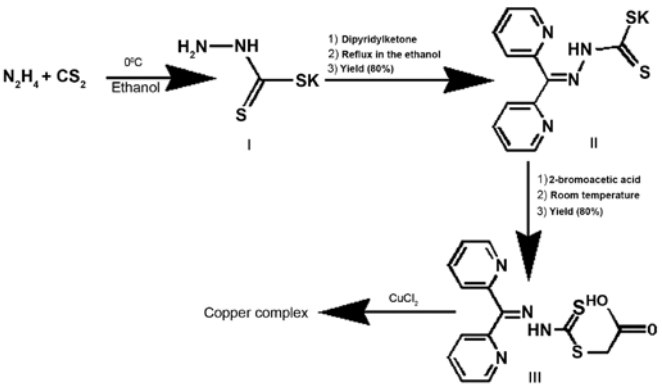

Figure 1. The synthetic route of DpdtaA and its copper complex. The conditions as indicated in the schedule.

Results

Preparation and proliferation inhibition of DpdtaA. A three-step reaction as described in Fig. 1 was used to generate the DpdtaA. Firstly, hydrazine reacted with carbon disulfide to form hydrazine dithiocarbamate (HdtC, I), then following addition of dipyridineketone, the dipyridylhydrazone dithiocarbamate (DpdtC, II) was made as previously described (19). The DpdtaA (III) was prepared by DpdtC reaction with 2-bromoacetic acid. The new compound was traced by TLC, purified by flash chromatography. Finally, the chemical structure of DpdtaA was characterized by NMR and HRMS spectra. HPLC and NMR showed that agents have adequate purity (>98%, data not shown), indicating that the new prepared DpdtaA can be used for biological assay.

We are interested in the biological activity of new synthetic DpdtaA, thus, antiproliferative activity of DpdtaA against hepatocellular carcinoma cell lines was screened (Fig. 2F-G), the dose-response curves are depicted in Fig. 2. As shown in Fig. 2F-G, DpdtaA exhibited significant growth inhibition for HepG2 and Bel-7402 (IC_{50} ≤6 μM), but the cell line dependence in dose-response was also obvious. For HepG2 cells, the maximal inhibition of ~80% can be achieved at 12.5 μM (Fig. 2F), but only 40% inhibition for Bel-7402 at the same concentration of DpdtaA (Fig. 2G). In view of the important role of copper ion in dithiocarbamates activity, the proliferation inhibition of DpdtaA in the presence of copper ion was also investigated. As previously reported, an antagonistic effect in growth inhibitions was observed for both cell lines, leading to an ~3-fold decrease in HepG2 cells based on IC_{50} value, but this was not evident for Bel-7402 cells except maximal inhibition, which was few for dithiocarbamate derivatives. To gain details, the morphologic change was further investigated. As shown in Fig. 2A-D, the DpdtaA caused rounded HepG2 cells, but the addition of copper ion

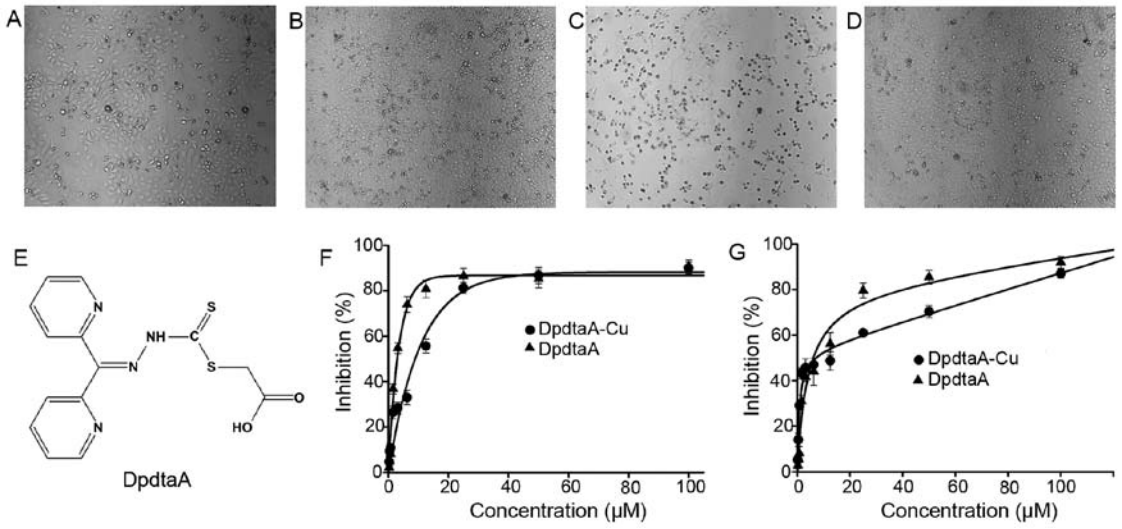

Figure 2. The chemical structures of DpdtaA and proliferation inhibition assay. The effect of DpdtaA and DpdtaA-Cu on morphology of HepG2 cells. (A) 1.56 μM DpdtaA after 24-h treatment; (B) 1.56 μM DpdtaA-Cu after 24-h treatment; (C) 3.12 μM DpdtaA after 24-h treatment; (D) 3.12 μM DpdtaA-Cu after 24-h treatment. (E) structure of DpdtaA; (F) proliferation inhibition of DpdtaA or its copper complex against HepG2 cell, IC_{50} = 3.0±0.4 μM for DpdtaA, 9.3±0.6 μM for its copper; (G) proliferation inhibition of DpdtaA or its copper complex against Bel-7402 cell, IC_{50} = 6.1±0.6 μM for DpdtaA, 6.6±0.3 μM for its copper.

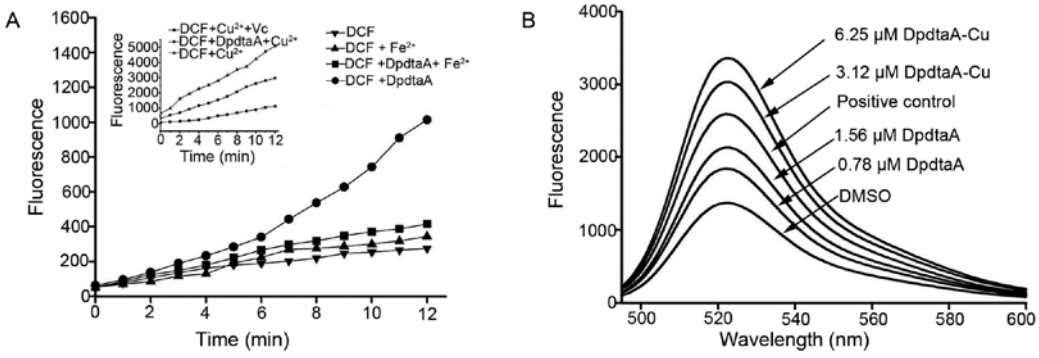

Figure 3. DpdtaA and its copper complex induces ROS generation *in vitro* and in cell level. (A) *In vitro* ROS generation by iron or copper (insert) involved Fenton-like reaction, the ROS content was measured by DCF fluorescence; (B) *in vivo* (cell level), the ROS production after exposure of the DpdtaA and its copper complex. The DMSO and positive control were also included.

significantly attenuated the action, showing an antagonistic effect as we previously reported (19). We speculated that the 'antagonistic effect' might stem from a new species which was confirmed at DpdtaA/Cu =1:1 ratio in composition by spectral titration (data not shown).

DpdtaA and its copper complex (DpdtaA-Cu) induces ROS generation. It is prevailingly accepted concept that antiproliferation inhibition (or cytotoxicity) of many drugs stem from generation of reactive oxygen species (ROS). DpdtaA may chelate iron or copper, thus, involved in Fenton or Fenton-like reaction. The ROS production *in vitro* is shown in Fig. 3A, fluorescence intensities of DCF in the presence of DpdtaA and Fe^{2+} was higher than that of Fe^{2+}, indicating that iron DpdtaA complex is redox active and could produce more ROS. In contrast, DpdtaA-Cu has weaker ability to generate ROS, however, in the reduced environment [presence of ascorbic acid (Vc)], the DpdtaA-Cu induced highest content of ROS. To further confirm the *in vitro* results, the drugs inducing intracellular ROS were investigated, as shown in Fig. 3B, both DpdtaA and its copper complex induced ROS generation in a concentration-dependent manner. It was noted that the fluorescent intensities of DCF from copper complex treated cells were significantly greater than that of DpdtaA, which might be related to the redox feature of $Cu^{2+/1+}$ complexes, because the copper (I) complex could also react with oxygen molecule to form superoxide radical except with H_2O_2 (25).

ROS mediates proliferative inhibition. As mentioned above, both DpdtaA and its copper complex induced ROS generation, whether the ROS generation was involved in antiproliferative activity was unclear. Thus, the correlation between ROS and growth inhibition, the effect of reducing agent, N-acetylcysteine (NAC) on growth inhibition of DpdtaA was investigated. The morphologic changes induced by DpdtaA in the absence or presence of NAC are shown in Fig. 4. It was clear that the numbers of rounded cells after addition of DpdtaA were decreased with increasing NAC (Fig. 4A-C), indicating that the NAC can protect the HepG2 cells from ROS oxidative damage. However, a contrary phenomenon in the

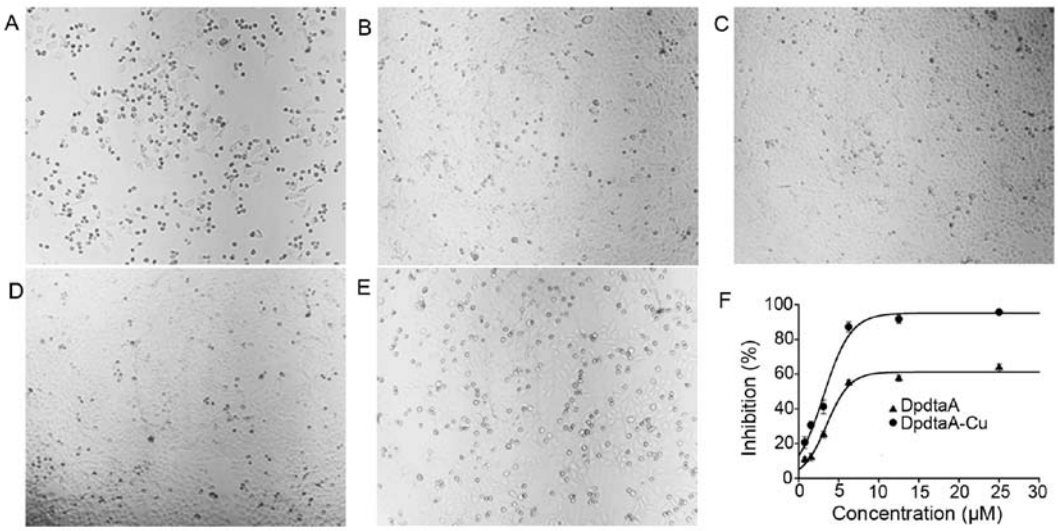

Figure 4. The effect of NAC on HepG2 cell growth inhibition of DpdtaA and its copper complex. (A) 3.12 μM DpdtaA; (B) 3.12 μM DpdtaA plus 0.5 mM NAC; (C) 3.12 μM DpdtaA plus 1.5 mM NAC; (D) 12.5 μM DpdtaA-Cu; (E) 12.5 μM DpdtaA-Cu plus 0.5 mM NAC; (F) growth inhibition of DpdtaA and DpdtaA-Cu in the presence of 2 mM NAC, IC_{50} = 5.5±0.6 μM for DpdtaA and 3.3±0.4 μM for DpdtaA-Cu.

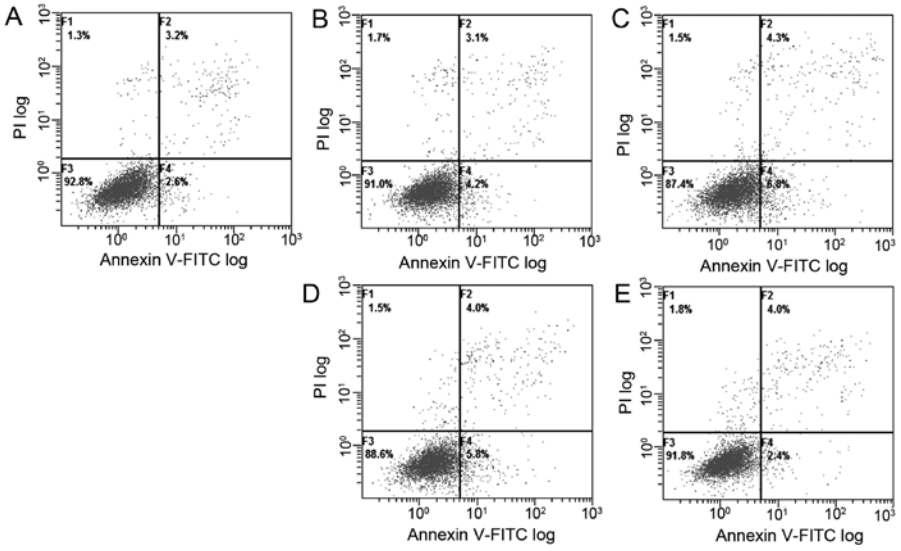

Figure 5. Flow cytometric analysis of apoptosis of HepG2 cells. DMSO, DpdtA and DpdtA-Cu were incubated with the cells for 24 h. All attached cells were collected and double stained with Annexin V and propidium iodide (PI) using a kit from Dojindo Laboratories following the manufacturer's instructions. (A) DMSO (control); (B) 0.78 M DpdtaA; (C) 1.56 μM DpdtaA; (D) 3.12 μM DpdtaA-Cu; (E) 6.25 μM DpdtaA-Cu.

DpdtaA-Cu treated cells was also observed, i.e., rounded cells increased (Fig. 4D-E) with addition of NAC. The situation was speculated to attribute to the redox feature of Cu^{2+} which can be reduced to Cu^{1+} by NAC, and the resulting DpdtaA-Cu^{1+} reacted with O_2 to generate more ROS. To confirm the speculation, the growth inhibition in the presence of NAC was further evaluated. As shown in Fig. 4F, the antiproliferative activity of DpdtaA was significantly decreased from ~90 to 60%, but the growth inhibition of DpdtaA-Cu dramatically increased, indicating the antiproliferative action of the agents was ROS mediated.

DpdtaA and its copper complex induce partly cellular apoptosis. It has been well documented that the excess intracellular ROS induce apoptosis whether the ROS induced by the agents involved in apoptosis was required to be determined. To measure the apoptosis populations at early and late stages, the Annexin V/propidium iodide (PI) staining was performed, which measures externalization of phosphatidylserine on the cell surface of apoptotic cells specifically. The flow cytometric analyses showed that the DpdtaA induced early apoptosis and later apoptosis in a concentration-dependent manner (Fig. 5A-C, from 5.8 to 11.1%), but the apoptotic ratios were smaller after 24-h treatment of DpdtaA. Similar situation for DpdtaA-Cu, just the percentage was less (5.8-9.8%) even at higher concentration.

Generally the excess ROS lead to apoptosis frequently signaling through changes in the expression of bcl-2 family proteins. To further support that the growth inhibition may involve apoptosis, the expressions of apoptosis related proteins were investigated by western blotting. The alterations of bcl-2

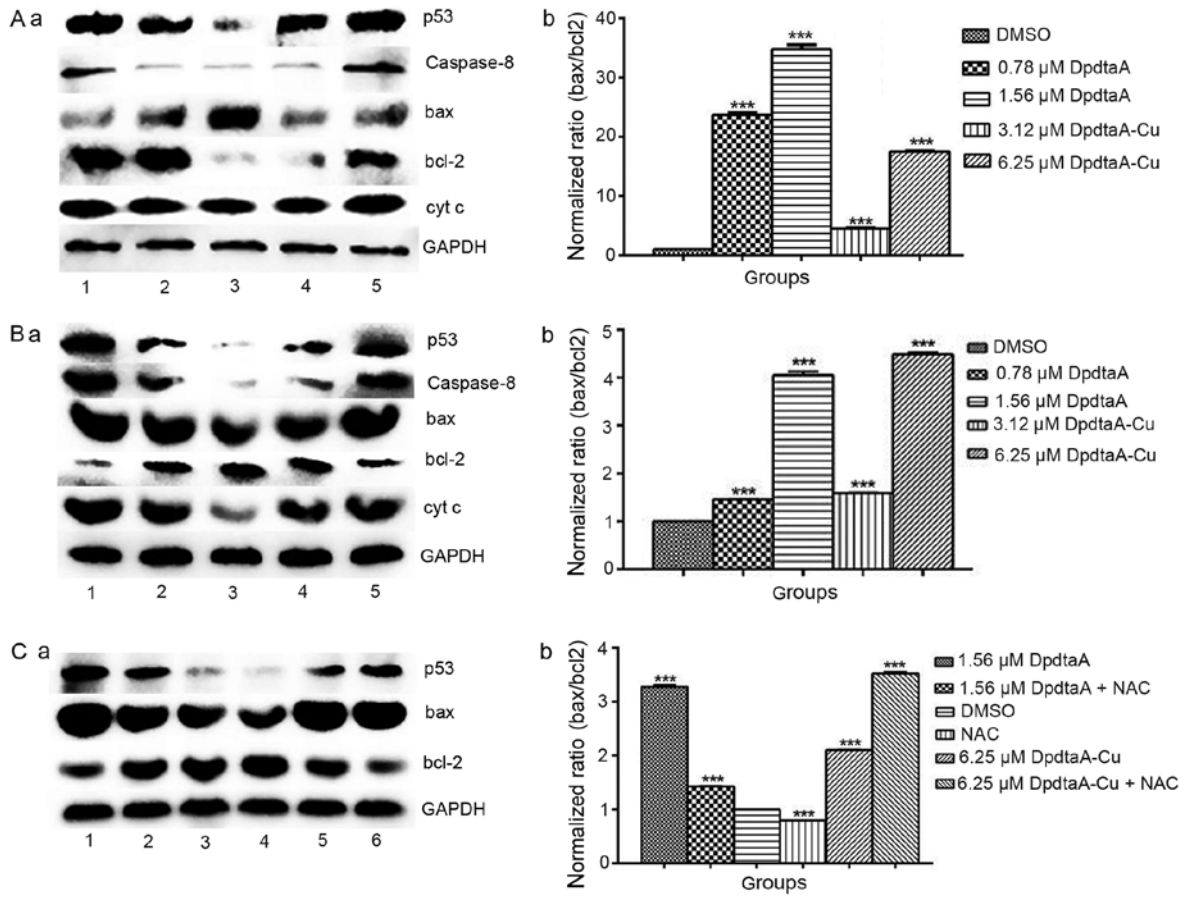

Figure 6. Western blot analysis of changes of apoptosis-related genes. (A-a) The changes of apoptosis-related protein in HepG2 cells, (A-b) normalized ratio of bax/bcl2; (B-a) the expression of apoptosis-related protein in Bel-7402 cells, (B-b) normalized ratio of bax/bcl2; lane 1, 1.56 μM DpdtaA; lane 2, 0.78 μM DpdtaA; lane 3, DMSO; lane 4, 3.12 μM DpdtaA-Cu; lane 5, 6.25 μM DpdtaA-Cu. (C-a) The effect of NAC on apoptosis-related protein in Bel-7402 cells, (C-b) normalized ratio of bax/bcl; lane 1, 1.56 μM DpdtaA; lane 2, 1.56 μM DpdtaA plus NAC; lane 3, DMSO; lane 4, NAC; lane 5, 6.25 μM DpdtaA-Cu; lane 6, 6.25 μM DpdtaA-Cu plus NAC. (***P<0.01; one-way ANOVA).

and bax proteins before and after treatment with DpdtaA at different concentrations were recorded (Fig. 6). It was clear that the increased bax was observed in both DpdtaA and DpdtaA-Cu treated HepG2 and Bel-7402 cells compared to that of control (Fig. 6A-a and B-a), on the contrary bcl-2, a pro-survival protein was downregulated in the agent treated cells. For comparative purposes, the ratio of bax/bcl-2 was normalized (Fig. 6A-b and B-b). As shown in Fig. 6A-b the difference in ratio of bax/bcl-2 was obvious, 23-35-fold increase for DpdtaA, 4- to 17-fold for DpdtaA-Cu. Similar results were observed in Bel-7402 cells except smaller folds (Fig. 6B-b). The increased bax/bcl2 determined that apoptosis occurred when the cells were treated with the agents. To correlate the apoptosis with ROS, the ROS scavenger NAC was added to the Bel-7402 cells either individually or combined. As shown in Fig. 6C-a, the NAC did decrease the ratio of bax/bcl2 compared to the DpdtaA (DpdtaA-Cu) treated group only, indicating that the agent-induced apoptosis was ROS-dependent.

The change of permeability of the mitochondria and cytochrome *c* release from the mitochondria are a key step in the process of apoptosis and is one of markers in intrinsic apoptosis, the increase of cytochrome *c* in cytoplasm (Fig. 6A-a and B-a), indicating that intrinsic apoptosis was involved in the growth inhibition induced by the agents. To determine whether apoptosis was due to p53 regulation, the expression of p53 was assessed, as shown in Fig. 6, the upregulated p53 may hint that there was a correlation between p53 and apoptosis. On the other hand, the upregulation of caspase-8 may also indicate that an extrinsic pathway protease was involved.

p53 upregulation correlate with downregulation of Mdm2 and disruption interaction between p53 and Mdm2 when exposing the agents to HepG2 cells. The DpdtaA and its copper complex induced alterations in apoptosis related proteins in both cell lines were similar, and could upregulate p53. Hence, the role of p53 required to be further investigated. Pifithrin-α (PFT-α) is a specific wild-type p53 inhibitor, and the expression of wild-type p53 in HepG2 cells was monitored in the presence or absence of 10 μM PFT-α. Western blot analysis revealed that the expression of p53 was significantly attenuated by PFT-α treatment or combination with the agents, compared with the treatment of agents alone (Fig. 7A). These results indicate that p53 played a role in agent-induced apoptosis. It has been accepted that cellular p53 levels is primarily controlled through its ubiquitin-mediated proteasomal degradation (26,27) and the mouse double minute protein 2 (Mdm2) as the principal endogenous E3-ligase with high specificity for p53 (28). The interaction of Mdm2 with p53 led to p53 degradation. Thus, the assessment of expression of Mdm2 was necessary. As shown in

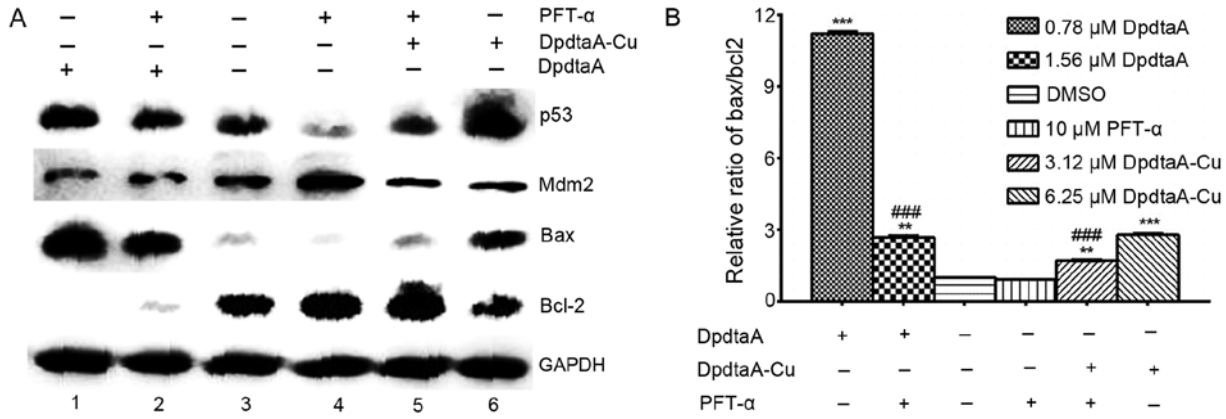

Figure 7. DpdtaA and its copper complex induces autophagy in HepG2 cells. Lane 1, 1.56 μM DpdtaA; lane 2, 1.56 μM DpdtaA plus 10 μM PFT-α; lane 3, DMSO; lane 4, 10 μM PFT-α; lane 5, 6.25 μM DpdtaA-Cu plus 10 μM PFT-α; lane 6, 6.25 μM DpdtaA-Cu (**P<0.05; ***P<0.01); $^{###}$P<0.01, one-way ANOVA).

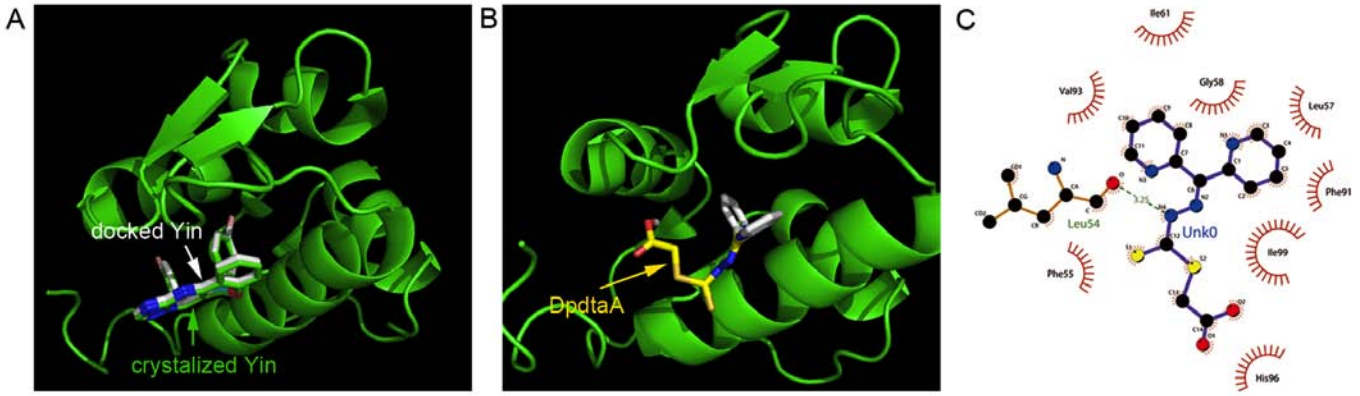

Figure 8. The interaction of DpdtaA with Mdm2. (A) Superimposed docked Yin on the crystallized Yin in Mdm2. (B) DpdtaA docked in Mdm2. (C) Interaction of DpdtaA with residues in the binding cavity (in the figure Unk0 = DpdtaA). Dark green dash lines (C) indicate hydrogen bonds. The eye-like curved dark red lines represent the hydrophobic residues in contact.

Fig. 7A, the downregulation of Mdm2 was observed in treatment of the cell with the agents, indicating that DpdtaA and its copper complex upregulated p53 via Mdm2 downregulation pathway. Since p53 exerts its induction of apoptosis mainly through the regulation of bcl-2 family proteins, the bcl-2 and bax protein levels were assessed. The relative ratio of bax/bcl-2 is shown in Fig. 7B, such ratio may determine the cell sensitivity or resistance to the apoptotic stimuli (7). On the other hand, p53 and Mdm2 interacted reciprocally, the interaction is hydrophobic interaction, disrupting the interaction would benefit the upregulation of p53. It has been demonstrated that some of small molecules can disrupt their interaction (29), so the theoretical simulation by molecular docking was conducted. The crystal structure of human type Mdm2 (PDB ID: 3jzk) was from the RCSB Protein Data Bank. In order to evaluate the accuracy of our docking protocol, the Yin (ligand in 3jzk) was re-docked into the Mdm2 complexes based on recommended procedure (Fig. 8A). As shown in Fig. 8, the docked Yin was almost fully superimposed on the native co-crystallized one. Thus, following the same protocol the DpdtaA was individually docked into the Mdm2 (Fig. 8B), the simulating affinity energies were -9.4 for Yin and -6.9 kcal/mol for DpdtaA, respectively. The interaction of DpdtaA with residues of Mdm2 is depicted in Fig. 8C. The data implied that the medium interaction between DpdtaA and Mdm2 might also contribute to the upregulation of p53.

DpdtaA and its copper complex leads to autophagy response. Previous report revealed that bax could be translocated from the cytosol to the lysosomal membrane, which led to alteration in lysosomal membrane integrity (30). To test this hypothesis, LysoTracker Red, which can accumulate within the lysosomes, was employed to assess the LMP (31). As shown in Fig. 9A-C, the treatments of DpdtaA and DpdtaA-Cu significantly increased the red fluorescence density in HepG2 cells compared to without treatment, indicating that LMP was altered. Furthermore, the changes in LMP may be a response to autophagy; thus, the formation of autophagosomes was measured by acridine orange staining. As shown in Fig. 9D, E and G, the accumulated red granular fluorescence in the acidic vacuoles was observed in the agent-treated groups, implying that the formation of autophagosome was increased, and autophagy occurred. To support the above conclusion, an autophagy inhibitor, 3-methyladenin (3-MA) was added to agent-treated cells and clearly the red granular fluorescence in the acidic vacuoles decreased compared to that the agent only (Fig. 9F and H). The LC3 (microtuble-associated protein

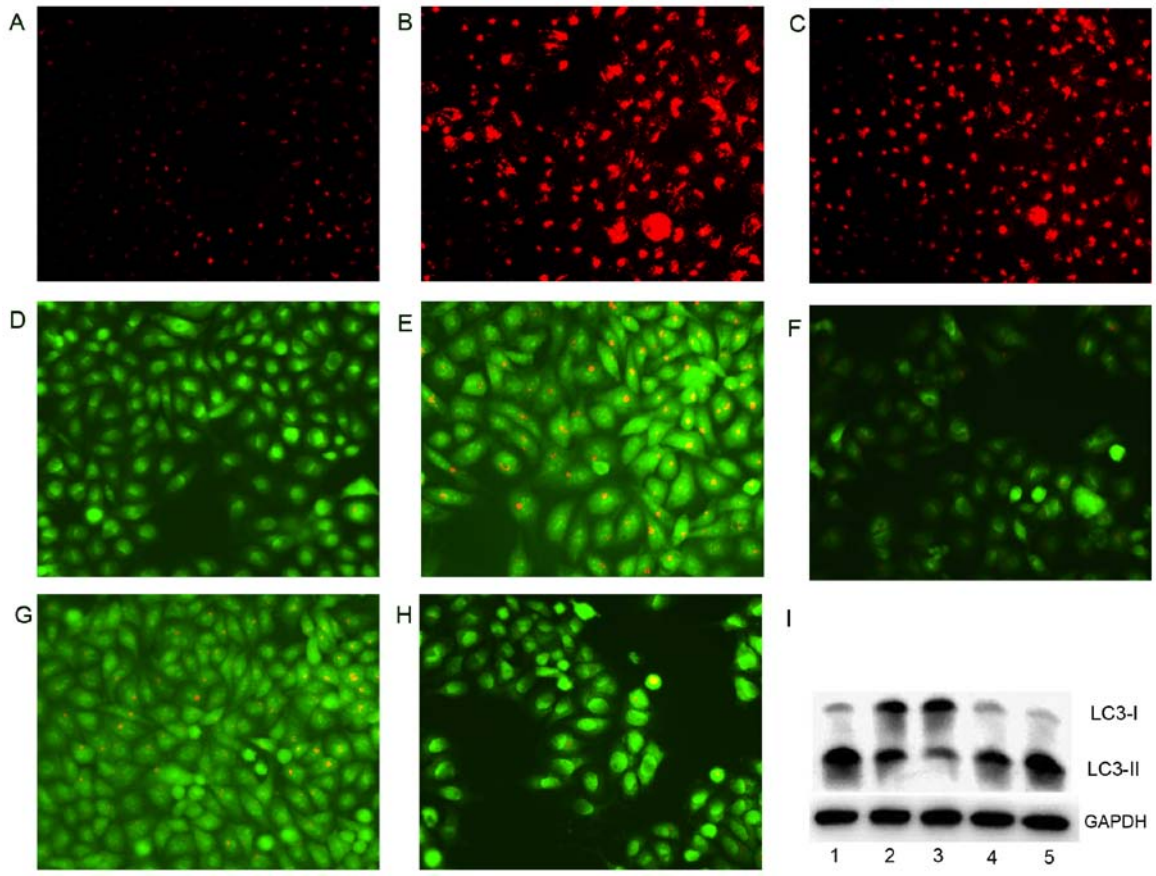

Figure 9. DpdtaA and its copper complex induces lysosomal membrane permeability and autophagy in HepG2 cells. Lysosomal membrane permeability (LysoTracker Red stained): (A) control; (B) 1.56 μM DpdtaA; (C) 6.25 μM DpdtaA-Cu. Acidic vacuoles in autophagosome (acridine orange): (D) DMSO; (E) 1.56 μM DpdtaA; (F) 1.56 μM DpdtaA plus 3-MA (2 mM); (G) 6.25 μM DpdtaA-Cu; (H) 6.25 μM DpdtaA-Cu plus 3-MA (2 mM); (I) western blotting: lane 1, 0.78 μM DpdtaA; lane 2, 1.56 μM DpdtaA; lane 3, DMSO; lane 4, 3.12 μM DpdtaA-Cu; lane 5, 6.25 μM DpdtaA-Cu.

light chain 3) is an autophagosome molecular marker, its change was further assessed by western blot analysis. As expected, the increase of cleaved LC3-II and decrease of LC3-I were observed compared to that of control, indicating that there was autophagy response after exposure of the agents (Fig. 9I). The changes of LC3-II were parallel to the results from acridine orange staining and demonstrated the DpdtaA and its copper complex had similar action in induction of autophagy.

Discussion

Tumor microenvironment plays an important role in tumor growth and metastasis (1,2), many proteases, metal ions and cytokine are located in ECM and maintain homeostasis of tumor environment. Once the homeostasis is disturbed, either overgrowth or growth inhibition will occur. On the other hand, cell proliferation requires some transition metals, and the demand in cancer cells is much higher than normal cells, therefore, moderate intervention of the metal homeostasis is valuable strategy in cancer therapy. The antitumor activity of dithiocarbamates, such as pyrrolidine dithiocarbamate (PDTC) is partly attributed to their metal chelation. The free thiol in dithiocarbamates is instable and thiol-alkylation may improve their stability (32). In the present study, pyridine ring and thioester structural units were introduced to dithiocarbamate in order to neutralize chelating ability and improve stability, and importantly enhance its antitumor activity. Chemotherapeutic drugs in cancer treatment normally correlate with the excess ROS production, that accordingly cause oxidative damage of protein and nucleic acids, resulting in cell death. In the present study the DpdtaA with similar ability to generate ROS both *in vitro* and *in vivo*, led to growth inhibition. ROS production induced by DpdtaA may involve in Fenton-like reaction [redox active DpdtaA-Fe^{2+}(Cu^{2+})] when endogenous agent chelate iron from iron labile pool (33). To determine whether the growth inhibition is ROS-dependent, an antioxidant, NAC was added during the proliferative assay, the attenuated growth inhibition clearly indicated that antiproliferative effect of DpdtaA was mediated by ROS, which is similar to that previously reported (34-36). Externalization of phosphatidylserine on the cell surface is one of apoptotic features, however, unexpectedly, the lower ratio of externalization was observed, which might be due to weaker activity of phospholipid scramblase induced by the agents. It is well known that in response to oxidative stress, the tumor suppressor p53 regulated expression of bcl-2 family and induced apoptosis (37). In the present study, DpdtaA upregulated p53 protein expression, downregulated antiapoptotic protein bcl-2 expression, promoting pro-apoptotic protein bax expression, triggering cell apoptosis via intrinsic and extrinsic pathway (Fig. 6) (38). Moreover, p53 can directly induce bax and bak oligomerization (39), thus, the higher ratio of bax/bcl-2 would be favorable for bax

oligomerization, consequently translocating the oligomerized bax to mitochondrial membrane, which lead to release of cytochrome *c* and caused mitochondrial cell death. p53 is a transcription factor, regulating many genes, including Mdm2, a p53 specific E3-ubiquitin-protein ligase. Thus, it was necessary to determine the expression of Mdm2. The results obtained from this study showed that the DpdtaA could downregulate Mdm2 expression, indicating that upregulation of p53 was partly due to Mdm2 feedback effect. Reversely blocking the p53 transcriptional activity by PFT-α could downregulate Mdm2 expression (Fig. 7). In addition to retroregulation of Mdm2, the dithiocarbamate bearing aromatic group might be a disruptor to intervene interaction between p53 and Mdm2. To probe the possibility, molecular docking was used, the simulation revealed the DpdtaA has a moderate affinity to Mdm2, implying that the disruption of the agents may not be excluded. The above indicated that DpdtaA-induced apoptosis in HepG2 cells mainly depended on p53-dependent pathway.

Autophagy occurs though degrading damaged proteins and/or organelles and recycling the materials to maintain the cell survival (40) and the acidic vesicular organelles (AVOs) is characteristic marker in the process (41). DpdtaA generated excess ROS that may trigger autophagy. The acidic vesicular organelles in stain of acridine orange was increased, the addition of an autophagy inhibitor (3-MA) could reverse this situation, clearly demonstrating that the antiproliferative activity of DpdtaA may be involved in autophagy. Further molecular evidence was gained from immunoblotting of LC3, the increased LC3-II were indicative of autophagy (Fig. 9F). It should be noted that autophagy can be either a physiological stress response or cytotoxically exerted, to distinguish the roles of autophagy in DpdtaA treatment, the autophagy inhibitor, 3-MA was employed, we found that the inhibitor (3-MA) could significantly enhance antiproliferative activity of DpdtA (data not shown), implying that the autophagy was stress induced, which was similar to that previously reported (42-44).

There are many catabolic enzymes in lysosome, its rupture can potentially be harmful to the cells. Massive lysosomal rupture causes release of lysosomal contents to cytoplasm and cytoplasmic acidification, consequently resulting in cell death [or lysosomal cell death (LCD)] (45). Therefore, the integrity of lysosomal membrane or LMP has important role in regulation of cell demise (46). Although the mechanism in LMP is not fully solved, some ways to destabilize the lysosomal membrane have been proposed: i) the compounds with detergent-like properties; ii) excess ROS; and iii) bax that can be translocated to lysosome membrane for pore formation, can destroy lysosomal membrane and lead to alteration in LMP (46,47). In the present study, the higher ratio of bax/bcl in DpdtaA group (Fig. 6) and more lysosomal dye in lysosome (Fig. 9) may indicate that antiproliferative effect of DpdtaA may also partly involve lysosomal cell death. In addition, there seemed to be a correlation between antiproliferation and LMP although it still questions the bax translocation to lysosome membrane (46,48).

Dithiocarbamates possess diverse biological activities, partly stemming from their metal chelating ability. *In vitro* copper complexes generally show an enhanced antiproliferative activity (13,20,21,49), but antagonistic effect was rarely reported. Dithiocarbamates can inhibit the canonical NF-κB pathway (50), but upon chelating with copper exhibit distinct biological activity (51). Dithiocarbamate copper complexes also show proteasome inhibition to display their cytotoxicity (52-54). However, the studies showed dithiocarbamates enhanced cytotoxicity upon chelation with copper ion. In the present study, we demonstrated that copper ion significantly attenuated antiproliferative activity of DpdtaA against HepG2 cells (Fig. 2), which was similar to that previously reported for DpdtpA (19). The two dithiocarbamtes (DpdtaA and DpdtpA) have similar structures, only one carbon difference, their antiproliferative effect against HepG2 cells was also similar, but upon chelation of copper, the propionic acid thiol ester showed greater fold decrease than acetate in antiproliferation. In addition, the copper complexes in composition were also different, ratio of DpdtpA/Cu was 2:1, but 1:1 for DpdtaA. Similar to previously reported, there was no correlation between cellular ROS level and its cytotoxicity (antiproliferation). DpdtaA-Cu has stronger ROS inducing ability *in vitro* and *in vivo*, but the changes in apoptotic proteins was not parallel, which violate currently accepted concept in ROS-based cancer therapy. This situation was also observed in the study by Zhu *et al* (55). However, the attenuated antiproliferative effect upon chelation of copper correlated with the lower ratio of bax/bcl and alteration in LMP (same concentration), indicating that copper ion may influence regulation of DpdtaA on bax gene expression.

In conclusion, DpdtaA stimuli caused ROS generation. In response to the oxidative stress, p53 was activated. More details revealed the upregulation of p53 stemmed from Mdm2 downregulation, attenuating degradation of ubiquitination of p53. Therefore antiproliferative activity exhibited by DpdtaA (or DpdtaA-Cu) was partly via p53 meditated apoptosis. In addition, the investigated agents also induced autophagy to respond the oxidative stress. Taken together, the autophagy lysosomal cell death and apoptosis were partly involved in antiproliferation of the agents. Yet, the paradoxical issue between ROS and cytotoxicity for DpdtaA-Cu and lesser extent of externalization of phosphatidylserine were not fully solved in mechanism and required further investigation.

Acknowledgements

The present study was supported by grants awarded by the Natural Science Foundation of China (no. 21571153), the Henan Science and Technology Agency (nos. 114300510012, 132102310250 and 152300410118), the Plan of Health Scientific and Technological Innovation Talents of Henan Province (no. 2109901) to S.L. and the Graduate innovation project of Xinxiang Medical University (YJSCX201613Y).

References

1. Spano D and Zollo M: Tumor microenvironment: A main actor in the metastasis process. Clin Exp Metastasis 29: 381-395, 2012.
2. Catalano V, Turdo A, Di Franco S, Dieli F, Todaro M and Stassi G: Tumor and its microenvironment: A synergistic interplay. Semin Cancer Biol 23: 522-532, 2013.
3. Sounni NE and Noel A: Targeting the tumor microenvironment for cancer therapy. Clin Chem 59: 85-93, 2013.
4. Khan G and Merajver S: Copper chelation in cancer therapy using tetrathiomolybdate: An evolving paradigm. Expert Opin Investig Drugs 18: 541-548, 2009.

5. Bogaard HJ, Mizuno S, Guignabert C, Al Hussaini AA, Farkas D, Ruiter G, Kraskauskas D, Fadel E, Allegood JC, Humbert M, *et al*: Copper dependence of angioproliferation in pulmonary arterial hypertension in rats and humans. Am J Respir Cell Mol Biol 46: 582-591, 2012.
6. Buac D, Schmitt S, Ventro G, Kona FR and Dou QP: Dithiocarbamate-based coordination compounds as potent proteasome inhibitors in human cancer cells. Mini Rev Med Chem 12: 1193-1201, 2012.
7. Li Y, Qi H, Li X, Hou X, Lu X and Xiao X: A novel dithiocarbamate derivative induces cell apoptosis through p53-dependent intrinsic pathway and suppresses the expression of the E6 oncogene of human papillomavirus 18 in HeLa cells. Apoptosis 20: 787-795, 2015.
8. Wang XJ, Xu HW, Guo LL, Zheng JX, Xu B, Guo X, Zheng CX and Liu HM: Synthesis and in vitro antitumor activity of new butenolide-containing dithiocarbamates. Bioorg Med Chem Lett 21: 3074-3077, 2011.
9. Mansouri-Torshizi H, Saeidifar M, Khosravi F, Divsalar A, Saboury AA and Hassani F: DNA binding and antitumor activity of α-diimineplatinum(II) and palladium(II) dithiocarbamate complexes. Bioinorg Chem Appl 2011: 394506, 2011.
10. Milacic V, Chen D, Ronconi L, Landis-Piwowar KR, Fregona D and Dou QP: A novel anticancer gold(III) dithiocarbamate compound inhibits the activity of a purified 20S proteasome and 26S proteasome in human breast cancer cell cultures and xenografts. Cancer Res 66: 10478-10486, 2006.
11. Nardon C, Schmitt SM, Yang H, Zuo J, Fregona D and Dou QP: Gold(III)-dithiocarbamato peptidomimetics in the forefront of the targeted anticancer therapy: Preclinical studies against human breast neoplasia. PLoS One 9: e84248, 2014.
12. Cattaruzza L, Fregona D, Mongiat M, Ronconi L, Fassina A, Colombatti A and Aldinucci D: Antitumor activity of gold(III)-dithiocarbamato derivatives on prostate cancer cells and xenografts. Int J Cancer 128: 206-215, 2011.
13. Schreck R, Meier B, Männel DN, Dröge W and Baeuerle PA: Dithiocarbamates as potent inhibitors of nuclear factor kappa B activation in intact cells. J Exp Med 175: 1181-1194, 1992.
14. Ronconi L, Marzano C, Zanello P, Corsini M, Miolo G, Maccà C, Trevisan A and Fregona D: Gold(III) dithiocarbamate derivatives for the treatment of cancer: Solution chemistry, DNA binding, and hemolytic properties. J Med Chem 49: 1648-1657, 2006.
15. Nobel CSI, Burgess DH, Zhivotovsky B, Burkitt MJ, Orrenius S and Slater AF: Mechanism of dithiocarbamate inhibition of apoptosis: Thiol oxidation by dithiocarbamate disulfides directly inhibits processing of the caspase-3 proenzyme. Chem Res Toxicol 10: 636-643, 1997.
16. Wu HH, Thomas JA and Momand J: p53 protein oxidation in cultured cells in response to pyrrolidine dithiocarbamate: A novel method for relating the amount of p53 oxidation in vivo to the regulation of p53-responsive genes. Biochem J 351: 87-93, 2000.
17. Wu HH and Momand J: Pyrrolidine dithiocarbamate prevents p53 activation and promotes p53 cysteine residue oxidation. J Biol Chem 273: 18898-18905, 1998.
18. Verhaegh GW, Richard MJ and Hainaut P: Regulation of p53 by metal ions and by antioxidants: Dithiocarbamate down-regulates p53 DNA-binding activity by increasing the intracellular level of copper. Mol Cell Biol 17: 5699-5706, 1997.
19. Wang T, Fu Y, Huang T, Liu Y, Wu M, Yuan Y, Li S and Li C: Copper ion attenuated the antiproliferative activity of di-2-pyridylhydrazone dithiocarbamate derivative; however, there was a lack of correlation between ROS generation and antiproliferative activity. Molecules 21: 1088, 2016.
20. Yang Y, Li C, Fu Y, Liu Y, Zhang Y, Zhang Y, Zhou P, Yuan Y, Zhou S, Li S, *et al*: Redox cycling of a copper complex with benzaldehyde nitrogen mustard-2-pyridine carboxylic acid hydrazone contributes to its enhanced antitumor activity, but no change in the mechanism of action occurs after chelation. Oncol Rep 35: 1636-1644, 2016.
21. Huang T, Li C, Sun X, Zhu Z, Fu Y, Liu Y, Yuan Y, Li S and Li C: The antitumor mechanism of di-2-pyridylketone 2-pyridine carboxylic acid hydrazone and its copper complex in ROS generation and topoisomerase inhibition, and hydrazone involvement in oxygen-catalytic iron mobilization. Int J Oncol 47: 1854-1862, 2015.
22. DeLano WL: The PyMOL Molecular Graphics System; DeLano Scientific, San Carlos, CA, USA, 2002.
23. Laskowski RA and Swindells MB: LigPlot+: Multiple ligand-protein interaction diagrams for drug discovery. J Chem Inf Model 51: 2778-2786, 2011.
24. Trott O and Olson AJ: AutoDock Vina: Improving the speed and accuracy of docking with a new scoring function, efficient optimization, and multithreading. J Comput Chem 31: 455-461, 2010.
25. Paris C, Bertoglio J and Bréard J: Lysosomal and mitochondrial pathways in miltefosine-induced apoptosis in U937 cells. Apoptosis 12: 1257-1267, 2007.
26. Brooks CL and Gu W: p53 ubiquitination: Mdm2 and beyond. Mol Cell 21: 307-315, 2006.
27. Kruse JP and Gu W: Modes of p53 regulation. Cell 137: 609-622, 2009.
28. Haupt Y, Maya R, Kazaz A and Oren M: Mdm2 promotes the rapid degradation of p53. Nature 387: 296-299, 1997.
29. Shangary S and Wang S: Small-molecule inhibitors of the MDM2-p53 protein-protein interaction to reactivate p53 function: A novel approach for cancer therapy. Annu Rev Pharmacol Toxicol 49: 223-241, 2009.
30. Johansson AC, Appelqvist H, Nilsson C, Kågedal K, Roberg K and Ollinger K: Regulation of apoptosis-associated lysosomal membrane permeabilization. Apoptosis 15: 527-540, 2010.
31. Rehman SU, Zubair H, Sarwar T, Husain MA, Ishqi HM, Nehar S and Tabish M: Redox cycling of Cu(II) by 6-mercaptopurine leads to ROS generation and DNA breakage: Possible mechanism of anticancer activity. Tumour Biol 36: 1237-1244, 2015.
32. Fussell KC, Udasin RG, Gray JP, Mishin V, Smith PJ, Heck DE and Laskin JD: Redox cycling and increased oxygen utilization contribute to diquat-induced oxidative stress and cytotoxicity in Chinese hamster ovary cells overexpressing NADPH-cytochrome P450 reductase. Free Radic Biol Med 50: 874-882, 2011.
33. Kello M, Drutovic D, Chripkova M, Pilatova M, Budovska M, Kulikova L, Urdzik P and Mojzis J: ROS-dependent antiproliferative effect of brassinin derivative homobrassinin in human colorectal cancer Caco2 cells. Molecules 19: 10877-10897, 2014.
34. Donadelli M, Dando I, Zaniboni T, Costanzo C, Dalla Pozza E, Scupoli MT, Scarpa A, Zappavigna S, Marra M, Abbruzzese A, *et al*: Gemcitabine/cannabinoid combination triggers autophagy in pancreatic cancer cells through a ROS-mediated mechanism. Cell Death Dis 2: e152, 2011.
35. Chripkova M, Zigo F and Mojzis J: Antiproliferative effect of indole phytoalexins. Molecules 21: 1626, 2016.
36. Gillardon F, Wickert H and Zimmermann M: Up-regulation of bax and down-regulation of bcl-2 is associated with kainate-induced apoptosis in mouse brain. Neurosci Lett 192: 85-88, 1995.
37. Amaral JD, Xavier JM, Steer CJ and Rodrigues CM: The role of p53 in apoptosis. Discov Med 9: 145-152, 2010.
38. Chen Y, Azad MB and Gibson SB: Methods for detecting autophagy and determining autophagy-induced cell death. Can J Physiol Pharmacol 88: 285-295, 2010.
39. Paglin S, Hollister T, Delohery T, Hackett N, McMahill M, Sphicas E, Domingo D and Yahalom J: A novel response of cancer cells to radiation involves autophagy and formation of acidic vesicles. Cancer Res 61: 439-444, 2001.
40. Lin J, Huang Z, Wu H, Zhou W, Jin P, Wei P, Zhang Y, Zheng F, Zhang J, Xu J, *et al*: Inhibition of autophagy enhances the anticancer activity of silver nanoparticles. Autophagy 10: 2006-2020, 2014.
41. Donohue E, Thomas A, Maurer N, Manisali I, Zeisser-Labouebe M, Zisman N, Anderson HJ, Ng SS, Webb M, Bally M, *et al*: The autophagy inhibitor verteporfin moderately enhances the antitumor activity of gemcitabine in a pancreatic ductal adenocarcinoma model. J Cancer 4: 585-596, 2013.
42. Zhang X, Xu Q, Zhang Z, Cheng W, Cao W, Jiang C, Han C, Li J and Hua Z: Chloroquine enhanced the anticancer capacity of VNP20009 by inhibiting autophagy. Sci Rep 6: 29774, 2016.
43. Serrano-Puebla A and Boya P: Lysosomal membrane permeabilization in cell death: New evidence and implications for health and disease. Ann N Y Acad Sci 1371: 30-44, 2016.
44. Aits S and Jäättelä M: Lysosomal cell death at a glance. J Cell Sci 126: 1905-1912, 2013.
45. Bové J, Martínez-Vicente M, Dehay B, Perier C, Recasens A, Bombrun A, Antonsson B and Vila M: BAX channel activity mediates lysosomal disruption linked to Parkinson disease. Autophagy 10: 889-900, 2014.
46. Guan JJ, Zhang XD, Sun W, Qi L, Wu JC and Qin ZH: DRAM1 regulates apoptosis through increasing protein levels and lysosomal localization of BAX. Cell Death Dis 6: e1624, 2015.
47. Fu Y, Yang Y, Zhou S, Liu Y, Yuan Y, Li S and Li C: Ciprofloxacin containing Mannich base and its copper complex induce antitumor activity via different mechanism of action. Int J Oncol 45: 2092-2100, 2014.

48. Oberle C, Huai J, Reinheckel T, Tacke M, Rassner M, Ekert PG, Buellesbach J and Borner C: Lysosomal membrane permeabilization and cathepsin release is a Bax/Bak-dependent, amplifying event of apoptosis in fibroblasts and monocytes. Cell Death Differ 17: 1167-1178, 2010.
49. Yang Y, Huang T, Zhou S, Fu Y, Liu Y, Yuan Y, Zhang Q, Li S and Li C: Antitumor activity of a 2-pyridinecarboxaldehyde 2-pyridinecarboxylic acid hydrazone copper complex and the related mechanism. Oncol Rep 34: 1311-1318, 2015.
50. Cvek B, Milacic V, Taraba J and Dou QP: Ni(II), Cu(II), and Zn(II) diethyldithiocarbamate complexes show various activities against the proteasome in breast cancer cells. J Med Chem 51: 6256-6258, 2008.
51. Cvek B and Dvorak Z: Targeting of nuclear factor-kappaB and proteasome by dithiocarbamate complexes with metals. Curr Pharm Des 13: 3155-3167, 2007.
52. Yu Z, Wang F, Milacic V, Li X, Cui QC, Zhang B, Yan B and Dou QP: Evaluation of copper-dependent proteasome-inhibitory and apoptosis-inducing activities of novel pyrrolidine dithiocarbamate analogues. Int J Mol Med 20: 919-925, 2007.
53. Skrott Z and Cvek B: Diethyldithiocarbamate complex with copper: The mechanism of action in cancer cells. Mini Rev Med Chem 12: 1184-1192, 2012.
54. Zhang H, Wu JS and Peng F: Potent anticancer activity of pyrrolidine dithiocarbamate-copper complex against cisplatin-resistant neuroblastoma cells. Anticancer Drugs 19: 125-132, 2008.
55. Zhu C, Hu W, Wu H and Hu X: No evident dose-response relationship between cellular ROS level and its cytotoxicity - a paradoxical issue in ROS-based cancer therapy. Sci Rep 4: 5029, 2014.